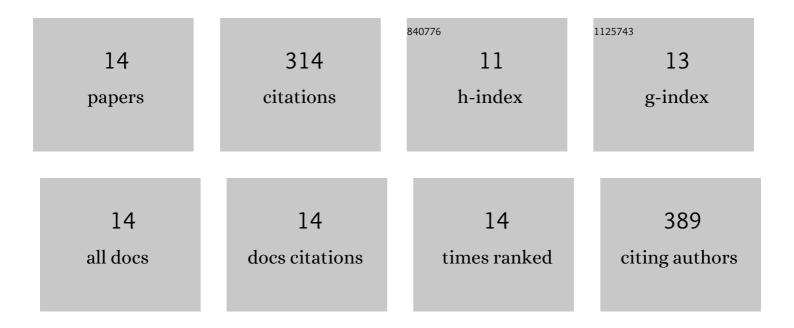
## **Chelsea Scott**

List of Publications by Year in descending order

Source: https://exaly.com/author-pdf/4255633/publications.pdf Version: 2024-02-01



| #  | Article  | IF   | CITATIONS |
|----|--|------|-----------|
| 1  | The <i>M</i> 7 2016 Kumamoto, Japan, Earthquake: 3â€Ð Deformation Along the Fault and Within the<br>Damage Zone Constrained From Differential Lidar Topography. Journal of Geophysical Research: Solid<br>Earth, 2018, 123, 6138-6155. | 3.4  | 75        |
| 2  | Structural data collection with mobile devices: Accuracy, redundancy, and best practices. Journal of Structural Geology, 2017, 102, 98-112.  | 2.3  | 59        |
| 3  | The 2016 M7 Kumamoto, Japan, Earthquake Slip Field Derived From a Joint Inversion of Differential Lidar<br>Topography, Optical Correlation, and InSAR Surface Displacements. Geophysical Research Letters, 2019,<br>46, 6341-6351.     | 4.0  | 30        |
| 4  | Surface materials and landforms as controls on InSAR permanent and transient responses to precipitation events in a hyperarid desert, Chile. Remote Sensing of Environment, 2020, 237, 111544.   | 11.0 | 23        |
| 5  | High-resolution surface faulting from the 1983 Idaho Lost River Fault Mw 6.9 earthquake and previous<br>events. Scientific Data, 2021, 8, 68.  | 5.3  | 23        |
| 6  | High-Detail Fault Segmentation: Deep Insight into the Anatomy of the 1983 Borah Peak Earthquake<br>Rupture Zone (Mw 6.9, Idaho, USA). Lithosphere, 2022, 2022, .   | 1.4  | 19        |
| 7  | Sensitivity of earthquake source inversions to atmospheric noise and corrections of InSAR data.<br>Journal of Geophysical Research: Solid Earth, 2016, 121, 4031-4044.   | 3.4  | 15        |
| 8  | Distribution of Aseismic Deformation Along the Central San Andreas and Calaveras Faults From<br>Differencing Repeat Airborne Lidar. Geophysical Research Letters, 2020, 47, e2020GL090628.   | 4.0  | 14        |
| 9  | Andean earthquakes triggered by the 2010 Maule, Chile (Mw 8.8) earthquake: Comparisons of geodetic, seismic and geologic constraints. Journal of South American Earth Sciences, 2014, 50, 27-39.                                       | 1.4  | 12        |
| 10 | Coseismic extension from surface cracks reopened by the 2014 Pisagua, northern Chile, earthquake sequence. Geology, 2016, 44, 387-390.   | 4.4  | 12        |
| 11 | Creep Along the Central San Andreas Fault From Surface Fractures, Topographic Differencing, and<br>InSAR. Journal of Geophysical Research: Solid Earth, 2020, 125, e2020JB019762.  | 3.4  | 12        |
| 12 | Measuring change at Earth's surface: On-demand vertical and three-dimensional topographic differencing implemented in OpenTopography. , 2021, 17, 1318-1332.   |      | 8         |
| 13 | Semiautomatic Algorithm to Map Tectonic Faults and Measure Scarp Height from Topography Applied to the Volcanic Tablelands and the Hurricane Fault, Western US. Lithosphere, 2022, 2021, .   | 1.4  | 6         |
| 14 | Statewide USGS 3DEP Lidar Topographic Differencing Applied to Indiana, USA. Remote Sensing, 2022, 14,<br>847.  | 4.0  | 6         |